nature structural & molecular biology

Interaction between FIP200 and ATG16L1 distinguishes ULK1 complex–dependent and –independent autophagy

Noor Gammoh, Oliver Florey, Michael Overholtzer & Xuejun Jiang

Autophagy is a finely orchestrated cellular catabolic process that requires multiple autophagy-related gene products (ATG proteins). The ULK1 complex functions to integrate upstream signals to downstream ATG proteins through an unknown mechanism. Here we have identified an interaction between mammalian FIP200 and ATG16L1, essential components of the ULK1 and ATG5 complexes, respectively. Further analyses show this is a direct interaction mediated by a short domain of ATG16L1 that we term the FIP200-binding domain (FBD). The FBD is not required for ATG16L1 self-dimerization or interaction with ATG5. Notably, an FBD-deleted ATG16L1 mutant is defective in mediating amino acid starvation–induced autophagy, which requires the ULK1 complex. However, this mutant retains its function in supporting glucose deprivation–induced autophagy, a ULK1 complex–independent process. This study therefore identifies a previously uncharacterized interaction between the ULK1 and ATG5 complexes that can distinguish ULK1-dependent and -independent autophagy processes.

Degradation of cellular contents can occur via the proteasome or lysosome systems[1]. There are a number of pathways that deliver substrates for degradation to either system. Macroautophagy (commonly referred to as autophagy) is one pathway that facilitates the degradation of long-lived proteins, damaged organelles and infectious pathogens, resulting in the clearance of toxic materials and increased nutrient availability in the cell[2]. Because of these substrates, autophagy has been implicated in a number of physiological and pathological processes including development, pathogen infection, neurodegeneration and cancer[3].

During autophagy, a number of protein complexes orchestrate the formation of a lipid bilayer (termed phagophore or pre-autophagosome), which, upon maturation, engulfs cytoplasmic materials and forms the autophagosome. The eventual fusion of autophagosomes with lysosomes results in degradation of the autophagosome contents and recycling of nutrients back into the cytoplasm. Key players in these events include a family of ubiquitin-like proteins, such as LC3, which are involved in phagophore maturation and possibly cargo selection[4–7]. Membrane targeting of LC3 is essential for autophagy and requires a series of ubiquitin-like conjugation events that lead to the conjugation of cytosolic LC3 (LC3-I) to the membrane-bound, phosphatidylethanolamine-conjugated form (LC3-II)[4]. These events are catalyzed by autophagy-related proteins (or ATG proteins) with E1-, E2- and E3-like enzymatic activities, termed ATG7, ATG3 and ATG5-ATG12, respectively. Formation of the ATG5-ATG12 conjugate (herein referred to as ATG5-12) is also catalyzed by similar conjugation events but requires a distinct E2-like enzyme termed ATG10 (ref. 8). In addition to its possible role as an E3-like enzyme during LC3-II formation, the ATG5-12 conjugate has been shown to form a large protein complex with ATG16L1, which is thought to be required to specify the site of LC3 conjugation during autophagy[9]. Depletion of any of ATG5, ATG16L1 or ATG7 completely abolishes autophagosome formation[10–12], whereas depletion of ATG3 results in defective maturation of the phagophore structure[13]. LC3 can also be recruited to single-membrane structures, for example during phagocytosis or entotic cell clearance[14–16]. In these cases, the core machinery used during LC3-II formation is also required.

A number of upstream signaling complexes can regulate autophagy, including the Vps34 and ULK1 complexes. The Vps34 complex comprises a number of proteins, including the Vps34 lipid kinase, p150, Beclin and ATG14, and is essential for phagophore formation and proper recruitment of ATG proteins to the phagophore[17,18]. The ULK1 complex, comprising the protein kinase ULK1 and several regulatory components including ATG13 and FIP200, is suppressed by mTORC1 kinase activity[19,20]. Once mTORC1 activity is inhibited, for example by amino acid deprivation or cytotoxic response, the ULK1 complex becomes activated and stimulates autophagy. Mechanistically, how the ULK1 complex coordinates with other ATG complexes during autophagy is not clear, and the protein substrate(s) of its kinase activity required for autophagy induction have not yet been identified.

In this study we sought to identify previously unknown players in autophagy that are particularly required during the initial stage of phagophore formation. To do so, we developed a system to isolate membrane-localized ATG proteins. Using this system, we conducted tandem affinity purification and identified FIP200 as a direct binding partner of ATG16L1. We further provide evidence that this

Cell Biology Department, Memorial Sloan Kettering Cancer Center, New York, New York, USA. Correspondence should be addressed to X.J. (jiangx@mskcc.org).

Received 11 October; accepted 26 November; published online 23 December 2012; corrected online 13 January 2013 (details online); doi:10.1038/nsmb.2475

previously uncharacterized interaction between the ULK1 complex and the ATG5 complex is required for ULK1 complex–dependent, but not ULK1 complex–independent, autophagy processes.

RESULTS

Pre-autophagosomes accumulate in the absence of ATG3

To study the molecular events during formation of the pre-autophagosome structures, we separated membrane-bound proteins from cytosolic proteins by subcellular fractionation. Cytosolic LC3 (LC3-I) was separated from membrane-bound LC3 (LC3-II) in wild-type mouse embryonic fibroblasts (MEFs; **Fig. 1a**). However, using this method, we scarcely detected the accumulation of upstream ATG proteins, such as ATG16L1, in the membrane fraction of wild-type MEFs even when autophagy was induced by amino acid deprivation (**Fig. 1b**). This suggests that the recruitment of upstream ATG proteins to pre-autophagosome structures may occur transiently. Previous studies suggest that in the absence of ATG3, pre-autophagosome structures are unable to mature into autophagosomes and therefore accumulate in the cell, probably leading to stabilization of upstream autophagy events that are transient in ATG3-expressing cells[13,21]. Therefore, we tested the subcellular localization of ATG16L1 in *Atg3*$^{-/-}$ MEFs. Notably, ATG16L1 accumulated in the membrane fraction of these cells (**Fig. 1b**). We detected no increase in ATG16L1 recruitment to the membrane fraction after 2 h of amino acid starvation in *Atg3*$^{-/-}$ cells, in agreement with previous studies[21]. Similarly, in immunofluorescence analyses we found that structures containing ATG16L1, which colocalized with endogenous ATG5, were detectable even under nutrient-rich conditions in the absence of ATG3 (**Fig. 1c**).

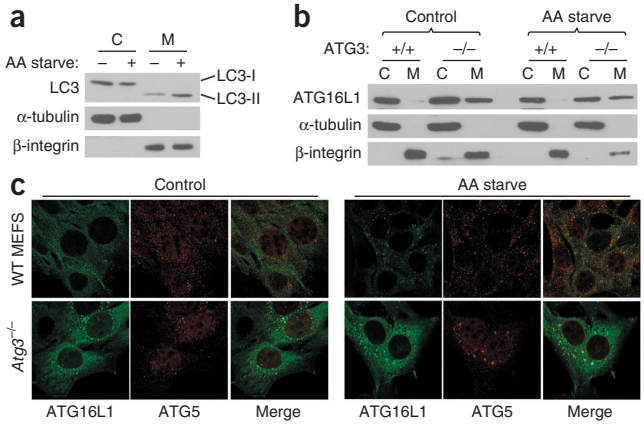

Figure 1 ATG16L1 stably localizes to membrane compartments in *Atg3*$^{-/-}$ cells. (**a**) Western blotting of membrane (M) and cytoplasmic (C) cell fractions of wild-type MEFs. Cells were either untreated (control) or incubated in amino acid–free medium for 2 h before harvesting (AA starve). Antibodies against α-tubulin and β-integrin were used as markers for cytosolic and membrane fractions, respectively. Antibodies against LC3 were used to verify localization of autophagosome structures to the membrane compartment. (**b**) Western blotting analysis of wild-type (+/+) or *Atg3*$^{-/-}$ (–/–) MEFs treated as in **a**. Note that ATG16L1 can stably localize to the membrane fraction only in *Atg3*$^{-/-}$ cells. (**c**) Immunofluorescence analysis of wild-type or *Atg3*$^{-/-}$ cells stably expressing S-tagged ATG16L1. Control or AA-starved cells, as in **a**, were fixed and stained with S tag–specific antibodies to detect ATG16L1 or with ATG5-specific antibodies. WT, wild type.

Identification of FIP200 as an ATG16L1-interacting partner

Next we sought to identify previously uncharacterized protein-protein interactions of membrane-bound ATG proteins in *Atg3*$^{-/-}$ cells using ATG14 and ATG16L1 as baits. For this, we used tandem affinity purification to purify ATG14 and ATG16L1 complexes followed by SDS-PAGE analysis and silver staining (**Fig. 2a**). We observed prominent bands in the ATG14 sample that correspond to known ATG14 interacting partners, including Vps34 and p150, confirming that functional autophagy complexes can be purified by this method. In the case of ATG16L1 purification, we detected a distinct band of a molecular weight greater than 170 kDa in addition to the ATG5-12 conjugate, the known binding partner of ATG16L1. Mass spectrometric analysis revealed the identity of this band as FIP200, an essential component of the ULK1 complex. Previously, the ULK1 complex has been proposed to be functionally linked to the ATG5 complex, but how these two complexes cross-talk is unclear.

To verify the interaction between ATG16L1 and FIP200, we expressed ATG16L1 in 293T cells and found that ATG16L1, but not ATG14, can pull down FIP200 as well as ATG13 (**Fig. 2b**). In addition, stably expressed ATG16L1 in *Atg3*$^{-/-}$ cells can also pull down endogenous FIP200, ATG13 and to a lesser extent ULK1 (**Supplementary Fig. 1a**). Reciprocal pull-downs of FIP200 expressed in 293T cells can coprecipitate ATG16L1 as well as the ATG5-12 conjugate (**Fig. 2c**). Furthermore, we tested whether endogenous FIP200 and ATG16L1 can interact with each other. Because their interaction is most likely transient and stabilized by ATG3 deletion, we used *Atg3*$^{-/-}$ cells for this purpose. We found that immunoprecipitation of endogenous FIP200 coprecipitated endogenous ATG16L1 in these cells (**Fig. 2d**). Using immunofluorescence analysis we observed that ATG16L1 punctate structures almost completely colocalized with FIP200 in both wild-type MEFs (**Fig. 2e**) and *Atg3*$^{-/-}$ cells (**Supplementary Fig. 1b**) as described previously[21,22].

Interaction between FIP200 and ATG16L1 is direct

Having shown that the ATG16L1-containing ATG5 complex and the FIP200-containing ULK1 complex can coprecipitate, we sought to determine which proteins directly mediate the interaction between these two complexes. First, we found that ATG16L1 and FIP200 can interact in MEF cells lacking the expression of ATG5 (**Fig. 3a** and **Supplementary Fig. 2a**) or ATG13 (**Fig. 3b**), indicating that ATG5 and ATG13 are dispensable for the interaction between ATG16L1 and FIP200. Furthermore, ATG5 and its ATG12 conjugation mutant (ATG5 K130R) were unable to pull down FIP200 (**Supplementary Fig. 2b**). In addition, we found that purified recombinant ATG16L1 can interact with recombinant FIP200 (**Fig. 3c**, left) but not with recombinant ATG13 (**Fig. 3c**, right) or with recombinant ATG3 or ATG7 (**Supplementary Fig. 2c**). Overall, these results indicate that ATG16L1 and FIP200 directly interact with each other independently of other complex components.

Identification of ATG16L1 domain required for FIP200 binding

To determine the function of the ATG16L1-FIP200 interaction in autophagy, we first sought to map the domain of ATG16L1 that is required to mediate binding to FIP200. We generated a series of ATG16L1 truncation fragments (**Fig. 4a**) based on previous structural analysis of yeast ATG16 (ref. 23–25). These include truncations of ATG16L1 that lack the N-terminal ATG5-binding region, the coiled-coil domain (CCD, required for self-dimerization), and seven WD40 repeats in the C-terminal half of ATG16L1. We expressed the truncation fragments of ATG16L1 in 293T cells and tested their interaction with endogenous FIP200 and ATG5. ATG16L1 fragments that were defective in ATG5 binding were still able to bind to FIP200 (**Fig. 4b**), indicating that FIP200 and ATG5 interact with ATG16L1 through distinct domains. The ATG16L1 fragment lacking a region between the WD40 and coiled-coil domains (Δ4 fragment,

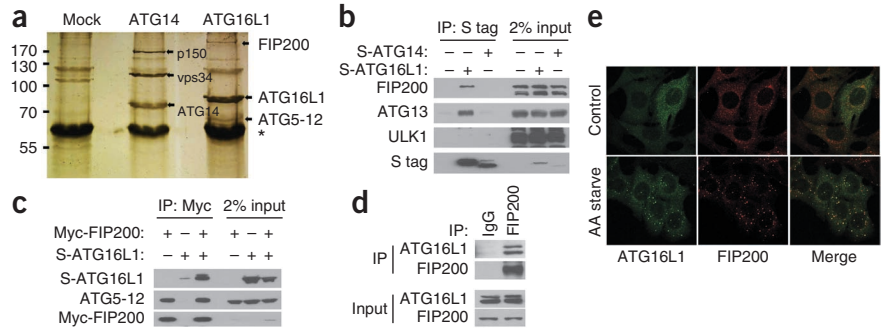

Figure 2 Identification of FIP200 as a binding partner of ATG16L1. (**a**) Silver staining was used to analyze protein complexes after tandem affinity purification from *Atg3*$^{-/-}$ cells stably expressing FLAG-S-tagged ATG14 or ATG16L1. (**b**) ATG16L1, but not ATG14, can interact with FIP200. Samples are whole-cell lysates from 293T cells expressing S-tagged ATG proteins and subjected to pull-downs using S-protein agarose. Bound proteins were analyzed by western blotting using antibodies against endogenous FIP200, ATG13 or ULK1. (**c**) Interaction between FIP200 and the ATG5-12–ATG16L1 complex in 293T whole-cell lysates. Cell lysates expressing Myc-FIP200 were subjected to immunoprecipitation with Myc-specific antibodies followed by western blotting analysis to detect S-tagged ATG16L1 and endogenous ATG5-12 conjugate. (**d**) Endogenous FIP200 and ATG16L1 can coimmunoprecipitate. Immunoprecipitation of endogenous FIP200 from *Atg3*$^{-/-}$ cells was followed by western blotting analysis to detect endogenous ATG16L1 binding. (**e**) ATG16L1 and FIP200 colocalize. Wild-type MEFs stably expressing GFP-ATG16L1 were left untreated (control) or incubated in the absence of amino acids (AA starve) for 2 h before fixation and immunofluorescence staining. FIP200-specific antibodies were used to stain for endogenous FIP200. Asterisk denotes IgG heavy chain.

residues 1–335 deleted) was defective in binding to FIP200. These results suggest that the interaction between ATG16L1 and FIP200 is mediated through residues 206–335 of ATG16L1. This region of ATG16L1 has previously been shown to be required for Rab33B binding[26].

The Δ4 fragment includes a large deletion of the N-terminal half of ATG16L1 and is therefore unable to bind ATG5 or self-dimerize, in addition to being unable to bind FIP200. Therefore, we sought to identify a smaller region of ATG16L1 that is required for FIP200 binding. By further mutational analyses we found that a region of ATG16L1 within residues 206–335 is required for FIP200 binding. Both an ATG16L1 mutant with these residues deleted (Δ229–242) and a mutant harboring a larger deletion (Δ182–242) were defective in binding to FIP200 compared to the full-length protein (**Fig. 4c**). However, the Δ229–242 mutant retained its ATG5 binding ability (**Fig. 4c**) as well as its ability to dimerize with full-length protein (**Fig. 4d**). Notably, residues 229–242 have previously been found dispensable for Rab33B binding[26]. In addition, these residues are not conserved in ATG16L2, which does not support autophagy despite its ability to self-dimerize and bind to ATG5 (ref. 26), but they are conserved in ATG16L1 from various vertebrate species (**Supplementary Fig. 3**). Consistent with this, we found that FIP200 was unable to bind ATG16L2 (**Fig. 4e**). These results demonstrate that residues 229–242 allow ATG16L1 to bind FIP200 but are not required for ATG16L1's binding to ATG5 or self-dimerization. We name this region the FIP200-binding domain (FBD) of ATG16L1.

ΔFBD mutant is defective in ULK1-dependent autophagy

To test whether the FIP200-ATG16L1 interaction is required for the function of ATG16L1 in autophagy, we reconstituted *Atg16l1*$^{-/-}$ MEFs with either full-length ATG16L1 or the FBD-deleted mutant (ΔFBD). In the absence of ATG16L1 expression, autophagy was completely disrupted[10]. When we expressed full-length ATG16L1 or ATG16L1ΔFBD, basal levels of autophagy were restored, as measured by conversion of LC3-I to LC3-II (**Fig. 5a**, lanes 3 and 5). However, when we induced autophagy by depriving cells of amino acids, ATG16L1ΔFBD-expressing cells showed greatly reduced autophagy compared to cells expressing full-length ATG16L1 (**Fig. 5a**, lanes 4 and 6). We obtained similar results when we induced autophagy by treating cells with the selective mTOR inhibitor Torin 1 (**Fig. 5b**). In addition, degradation of p62 (a well-established autophagosome substrate) was impeded in the ATG16L1ΔFBD-reconstituted cells (**Fig. 5c**), providing further evidence for the defect of ATG16L1ΔFBD in mediating amino acid starvation–induced autophagy. In contrast, we found that the ΔWD40 mutant, which retains its ability to bind to FIP200 (**Fig. 4b**), restored amino acid starvation–induced autophagy to levels similar to full-length protein (**Supplementary Fig. 4**). Consistent with this, ATG16L1ΔFBD showed reduced ability to localize to punctate structures corresponding to pre-autophagosomes (**Fig. 5d**). The formation of GFP-tagged LC3 punctate structures, a marker of autophagosomes, was also markedly reduced in cells reconstituted with ATG16L1ΔFBD compared to cells reconstituted with full-length ATG16L1 (**Fig. 5e**). Therefore, the FIP200-ATG16L1 interaction is crucial for the function of ATG16L1 during amino acid starvation–induced autophagy, a process that requires the FIP200-containing ULK1 complex.

ΔFBD mutant is fully active during ULK1-independent autophagy

The inability of ATG16L1ΔFBD to fully restore autophagy could be due to overall misfolding of the protein caused by the introduced truncation, rather than its deficiency in binding FIP200. If so, our results in **Figure 5** would not support functional relevance of the FIP200-ATG16L1 interaction. Therefore, we sought to assess whether ATG16L1ΔFBD has any autophagy-related function independent of FIP200 and, therefore, the ULK1 complex. Recently, it has been suggested that glucose starvation induces autophagy in a ULK1

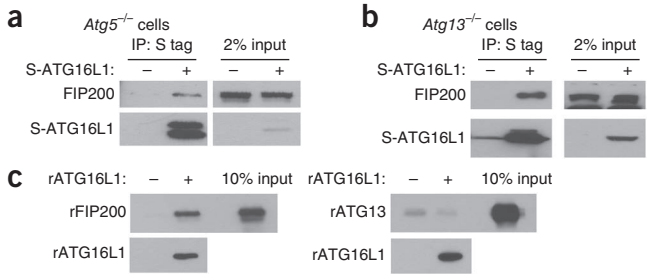

Figure 3 Interaction between ATG16L1 and FIP200 is direct. (**a**,**b**) Neither ATG5 nor ATG13 is required for interaction between ATG16L1 and FIP200. Lysates of *Atg5*$^{-/-}$ (**a**) or *Atg13*$^{-/-}$ MEFs (**b**) stably expressing S-tagged ATG16L1 (S-ATG16L1) were subjected to S-protein agarose pull-down followed by western blotting analysis using antibodies against FIP200 to detect binding to endogenous FIP200. (**c**) Interaction between purified recombinant FIP200 and ATG16L1. Recombinant ATG16L1 (rATG16L1) was incubated with either recombinant FIP200 (rFIP200; left) or recombinant ATG13 (rATG13; right). As negative controls, rFIP200 or rATG13 were incubated in the absence of rATG16L1 under identical conditions.

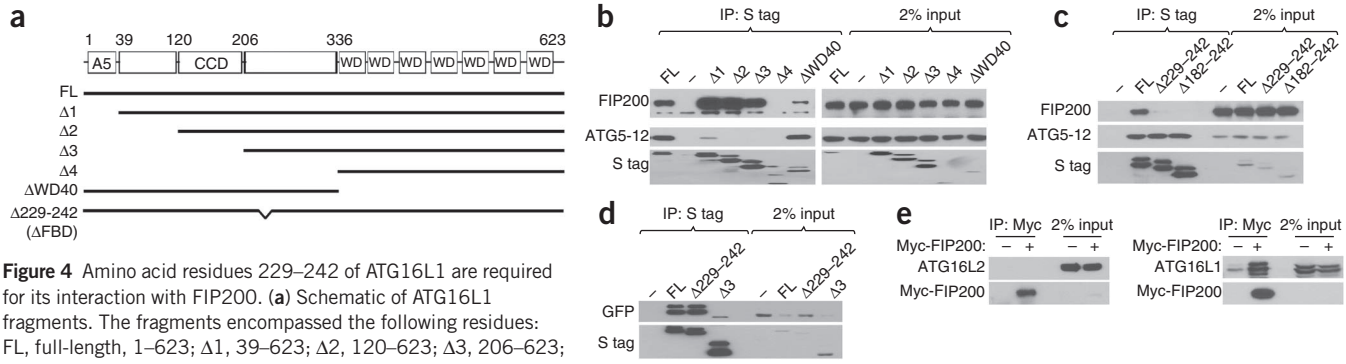

Figure 4 Amino acid residues 229–242 of ATG16L1 are required for its interaction with FIP200. (**a**) Schematic of ATG16L1 fragments. The fragments encompassed the following residues: FL, full-length, 1–623; Δ1, 39–623; Δ2, 120–623; Δ3, 206–623; Δ4, 336–623; ΔWD40, 1–335. The construct Δ229–242 lacks the FIP200-binding domain and is termed ΔFBD in subsequent figures. WD, WD40 repeats. (**b**,**c**) S-tagged ATG16L1 fragments (**b**), or S-tagged deletion mutants of ATG16L1 lacking residues 229–242 or 182–242 (**c**), were expressed in 293T cells. After S-protein agarose pull-downs, interaction with endogenous FIP200 and ATG5-12 was analyzed by western blotting. Residual binding of the Δ1 fragment to ATG5-12 is most likely due to dimerization with endogenous ATG16L1. (**d**) Full-length GFP-tagged ATG16L1 was coexpressed with S-tagged FL, Δ229–242 or Δ3 constructs, followed by S-protein agarose pull-down and western blotting. Note that the Δ3 mutant lacking the CCD is unable to self-dimerize. (**e**) 293T whole-cell lysate expressing Myc-tagged FIP200 was subjected to anti-Myc immunoprecipitation and western blotting analysis using antibodies against endogenous ATG16L2 (left) or ATG16L1 (right).

complex–independent manner that correlates with an increase in cellular ammonia levels and lack of mTORC1 inhibition[27,28]. We confirmed this using ULK1 and ULK2 double-knockout MEFs, in which glucose starvation induced formation of LC3-II that was susceptible to lysosomal degradation (**Fig. 6a**). We also observed that glucose starvation did not induce ULK1 dephosphorylation on residues that are dephosphorylated during amino acid starvation[29] (**Fig. 6b**). Notably, when we reconstituted *Atg16l1*$^{-/-}$ cells with full-length ATG16L1 or ATG16L1ΔFBD, we observed comparable conversion of LC3-I to LC3-II upon glucose starvation, whereas the absence of ATG16L1 expression completely abolished LC3 conjugation (**Fig. 6c**). This indicates that ATG16L1ΔFBD is fully functional during such ULK1 complex–independent autophagy. Similarly, we observed comparable formation of GFP-LC3 punctate structures in cells expressing full-length ATG16L1 or ATG16L1ΔFBD (**Fig. 6d**). Overall, these analyses suggest that, unlike ULK1 complex–dependent autophagy induced by amino acid starvation, ULK1 complex–independent autophagy induced by glucose starvation does not require FIP200 binding to ATG16L1.

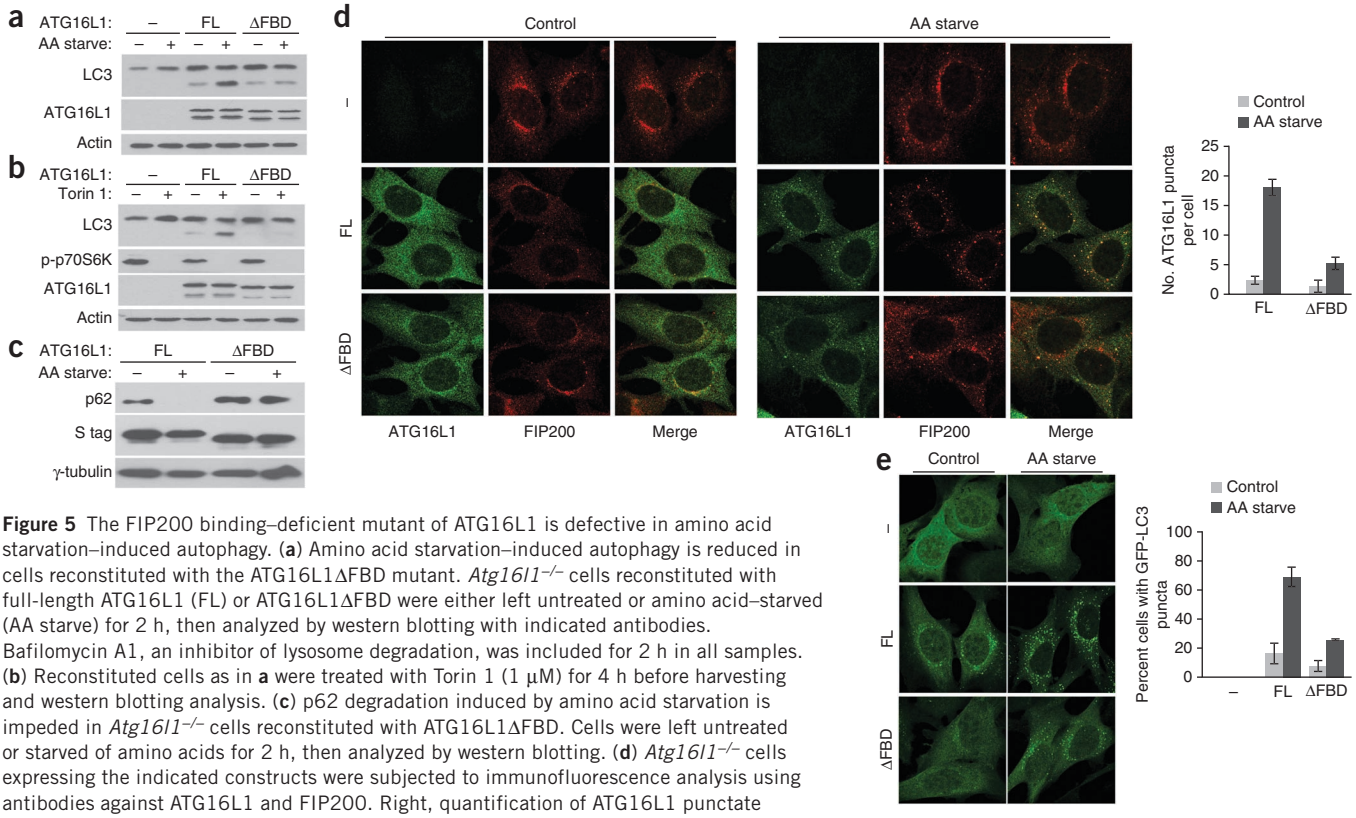

Figure 5 The FIP200 binding–deficient mutant of ATG16L1 is defective in amino acid starvation–induced autophagy. (**a**) Amino acid starvation–induced autophagy is reduced in cells reconstituted with the ATG16L1ΔFBD mutant. *Atg16l1*$^{-/-}$ cells reconstituted with full-length ATG16L1 (FL) or ATG16L1ΔFBD were either left untreated or amino acid–starved (AA starve) for 2 h, then analyzed by western blotting with indicated antibodies. Bafilomycin A1, an inhibitor of lysosome degradation, was included for 2 h in all samples. (**b**) Reconstituted cells as in **a** were treated with Torin 1 (1 μM) for 4 h before harvesting and western blotting analysis. (**c**) p62 degradation induced by amino acid starvation is impeded in *Atg16l1*$^{-/-}$ cells reconstituted with ATG16L1ΔFBD. Cells were left untreated or starved of amino acids for 2 h, then analyzed by western blotting. (**d**) *Atg16l1*$^{-/-}$ cells expressing the indicated constructs were subjected to immunofluorescence analysis using antibodies against ATG16L1 and FIP200. Right, quantification of ATG16L1 punctate structures per cell. Error bars show s.d. from three independent experiments with approximately 16 cells counted per condition. (**e**) GFP-LC3 expressed in *Atg16l1*$^{-/-}$ cells reconstituted with FL or ATG16L1ΔFBD and treated as in **d**. Right, quantification of GFP-LC3 punctate structures. Error bars show s.d. from three independent experiments.

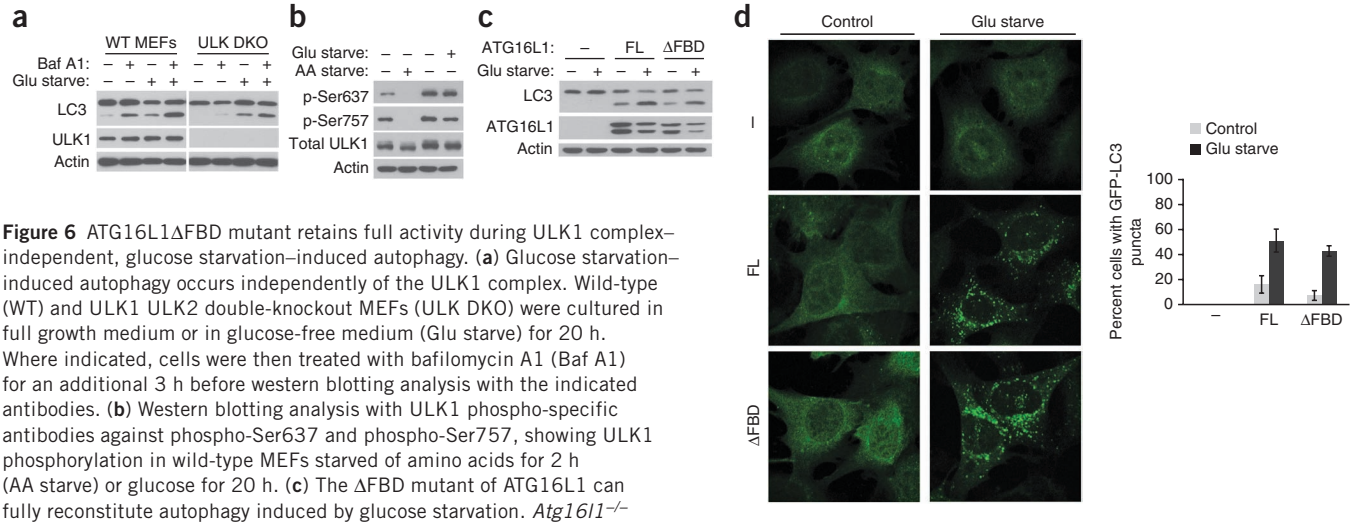

Figure 6 ATG16L1ΔFBD mutant retains full activity during ULK1 complex–independent, glucose starvation–induced autophagy. (**a**) Glucose starvation–induced autophagy occurs independently of the ULK1 complex. Wild-type (WT) and ULK1 ULK2 double-knockout MEFs (ULK DKO) were cultured in full growth medium or in glucose-free medium (Glu starve) for 20 h. Where indicated, cells were then treated with bafilomycin A1 (Baf A1) for an additional 3 h before western blotting analysis with the indicated antibodies. (**b**) Western blotting analysis with ULK1 phospho-specific antibodies against phospho-Ser637 and phospho-Ser757, showing ULK1 phosphorylation in wild-type MEFs starved of amino acids for 2 h (AA starve) or glucose for 20 h. (**c**) The ΔFBD mutant of ATG16L1 can fully reconstitute autophagy induced by glucose starvation. *Atg16l1*$^{-/-}$ cells reconstituted with full-length ATG16L1 (FL) or ΔFBD mutant were either left untreated or glucose-starved for 20 h, and samples were analyzed by western blotting with the indicated antibodies. (**d**) Fluorescence analysis of reconstituted cells as in **c** expressing GFP-LC3. Right, quantification of cells with GFP-LC3 punctate structures. Error bars show s.d. from three independent experiments. Approximately 400 cells were counted per condition.

DISCUSSION

In this study we offer evidence for a direct interaction between the ULK1 complex component FIP200 and the ATG5 complex component ATG16L1. The finding that this interaction is specifically required for ULK1 complex–dependent autophagy provides mechanistic insights into how the ULK1 complex communicates with other ATG complexes such as the ATG5 complex. The ATG5 complex (including its component ATG16L1) belongs to the essential core autophagy machinery, whereas the ULK1 complex seems to mediate autophagy induced by only certain specific triggers. The LC3 conjugation reaction is intact in cells with genetic deletion of ULK1 (refs. 30,31), and LC3-II formation takes place at basal levels in cells depleted of ULK1 complex components[22,32]. Moreover, the ULK1 complex, but not the ATG5 complex, is dispensable for glucose starvation–induced autophagy[27].

It would be interesting to consider whether ATG16L1 might be a convergence point mediating other upstream autophagy signals, in addition to signals through ULK1. It is evident, however, that the FBD region of ATG16L1 is not necessarily responsible for all other signals because ATG16L1ΔFBD is functionally intact during glucose starvation–induced autophagy. Another recognizable structure in ATG16L1 is the C-terminal WD40 repeats, a versatile protein-protein interaction domain that is not present in yeast ATG16. Although not required for autophagy triggered by amino acid starvation, it is possible that this region mediates certain other autophagy signals. If so, then the C-terminal region of ATG16L1 enables the mammalian autophagy pathway to sense more diverse and complex signals compared to its yeast counterpart. However, it is also possible that the WD40 repeats in mammalian ATG16L1 are relevant only to non-autophagy processes[10,33]. In light of this, it would be useful to explore the potential pathological role of the Crohn's disease–associated ATG16L1 mutation (T300A), which lies within the WD40 repeats, in both autophagy-related and non–autophagy-related processes[34,35].

A detailed comparison of ATG16L1 with its homolog ATG16L2 should also shed light on the function of ATG16L1 during autophagy. Unlike ATG16L1, ATG16L2 is unable to support autophagy or localize to the phagophore structures despite its ability to bind ATG5, self-oligomerize and form a large protein complex with the ATG5-12 complex[26]. ATG16L1 proteins from various vertebrate species all have highly conserved FBD regions, whereas ATG16L2 lacks this domain. Consistent with this, we found ATG16L2 did not interact with FIP200. However, whether the lack of FBD renders ATG16L2 inactive in autophagy is unclear, as ATG16L1 with its FBD deleted can still mediate ULK1 complex–independent autophagy. In addition, neither yeast nor *Caenorhabditis elegans* ATG16 have this domain (there is no true FIP200 homolog in these organisms either). Furthermore, previous *in vitro* biochemical studies suggest that yeast ATG16 is not required for the E3-like activity of ATG5-12 during the conjugation of ATG8 (the yeast homolog of LC3) to phosphatidylethanolamine[36]. Thus, in mammalian cells, the difference between ATG16L1 and ATG16L2 in autophagy does not seem to be due to their differential influence on the E3-like enzymatic activity of the ATG5 complex. The exact structural and biochemical mechanism that renders ATG16L1 but not ATG16L2 an essential functional component in autophagy has yet to be defined.

In conclusion, this study has uncovered a previously uncharacterized functional interaction between two upstream ATG complexes and has demonstrated that ATG16L1 is not only an essential structural component of the ATG5 complex but also a signaling protein that can mediate specific upstream signals during autophagy, such as those transduced by the ULK1 complex.

METHODS

Methods and any associated references are available in the online version of the paper.

Note: Supplementary information is available in the online version of the paper.

ACKNOWLEDGMENTS

We thank S. Akira (Osaka University) for *Atg16l1*$^{-/-}$ MEFs, M. Komatsu (Tokyo Metropolitan Institute of Medical Science) for *Atg3*$^{-/-}$ MEFs, N. Mizushima (Tokyo Medical and Dental University) for *Atg5*$^{-/-}$ MEFs, C. Thompson (Memorial Sloan Kettering Cancer Center, MSKCC) for ULK1 and ULK2 double-knockout MEFs, F. Giancotti (MSKCC) for β-integrin–specific antibody and H. Erdjument-Bromage (MSKCC) for mass spectrometric analyses. We thank members of the X.J. laboratory for critical reading of the manuscript and discussion. This work was supported in part by US National Institutes of Health (NIH) grants U54CA137788, R01CA113890 and R01CA166413 (to X.J.); US National Cancer Institute grant R01CA154649, the Benjamin Friedman Research Fund and the Louis V. Gerstner, Jr. Young Investigators Fund (to M.O.); and NIH fellowship 1F32CA162691 (to N.G.).

AUTHOR CONTRIBUTIONS
N.G. and X.J. designed the study and wrote the paper; N.G. and O.F. performed the experiments; N.G., O.F., M.O. and X.J. analyzed the data.

COMPETING FINANCIAL INTERESTS
The authors declare no competing financial interests.

Published online at http://www.nature.com/doifinder/10.1038/nsmb.2475.
Reprints and permissions information is available online at http://www.nature.com/reprints/index.html.

1. Ciechanover, A. Proteolysis: from the lysosome to ubiquitin and the proteasome. *Nat. Rev. Mol. Cell Biol.* **6**, 79–87 (2005).
2. Wirawan, E., Vanden Berghe, T., Lippens, S., Agostinis, P. & Vandenabeele, P. Autophagy: for better or for worse. *Cell Res.* **22**, 43–61 (2012).
3. Levine, B. & Kroemer, G. Autophagy in the pathogenesis of disease. *Cell* **132**, 27–42 (2008).
4. Geng, J. & Klionsky, D.J. The Atg8 and Atg12 ubiquitin-like conjugation systems in macroautophagy. 'Protein modifications: beyond the usual suspects' review series. *EMBO Rep.* **9**, 859–864 (2008).
5. Bjørkøy, G. *et al.* p62/SQSTM1 forms protein aggregates degraded by autophagy and has a protective effect on huntingtin-induced cell death. *J. Cell Biol.* **171**, 603–614 (2005).
6. Pankiv, S. *et al.* p62/SQSTM1 binds directly to Atg8/LC3 to facilitate degradation of ubiquitinated protein aggregates by autophagy. *J. Biol. Chem.* **282**, 24131–24145 (2007).
7. Kraft, C., Peter, M. & Hofmann, K. Selective autophagy: ubiquitin-mediated recognition and beyond. *Nat. Cell Biol.* **12**, 836–841 (2010).
8. Nemoto, T. *et al.* The mouse APG10 homologue, an E2-like enzyme for Apg12p conjugation, facilitates MAP-LC3 modification. *J. Biol. Chem.* **278**, 39517–39526 (2003).
9. Fujita, N. *et al.* The Atg16L complex specifies the site of LC3 lipidation for membrane biogenesis in autophagy. *Mol. Biol. Cell* **19**, 2092–2100 (2008).
10. Saitoh, T. *et al.* Loss of the autophagy protein Atg16L1 enhances endotoxin-induced IL-1β production. *Nature* **456**, 264–268 (2008).
11. Mizushima, N. *et al.* Dissection of autophagosome formation using Apg5-deficient mouse embryonic stem cells. *J. Cell Biol.* **152**, 657–668 (2001).
12. Komatsu, M. *et al.* Impairment of starvation-induced and constitutive autophagy in Atg7-deficient mice. *J. Cell Biol.* **169**, 425–434 (2005).
13. Sou, Y.S. *et al.* The Atg8 conjugation system is indispensable for proper development of autophagic isolation membranes in mice. *Mol. Biol. Cell* **19**, 4762–4775 (2008).
14. Florey, O., Kim, S.E., Sandoval, C.P., Haynes, C.M. & Overholtzer, M. Autophagy machinery mediates macroendocytic processing and entotic cell death by targeting single membranes. *Nat. Cell Biol.* **13**, 1335–1343 (2011).
15. Martinez, J. *et al.* Microtubule-associated protein 1 light chain 3 alpha (LC3)-associated phagocytosis is required for the efficient clearance of dead cells. *Proc. Natl. Acad. Sci. USA* **108**, 17396–17401 (2011).
16. Florey, O. & Overholtzer, M. Autophagy proteins in macroendocytic engulfment. *Trends Cell Biol.* **22**, 374–380 (2012).
17. Itakura, E., Kishi, C., Inoue, K. & Mizushima, N. Beclin 1 forms two distinct phosphatidylinositol 3-kinase complexes with mammalian Atg14 and UVRAG. *Mol. Biol. Cell* **19**, 5360–5372 (2008).
18. Zhong, Y. *et al.* Distinct regulation of autophagic activity by Atg14L and Rubicon associated with Beclin 1-phosphatidylinositol-3-kinase complex. *Nat. Cell Biol.* **11**, 468–476 (2009).
19. Ganley, I.G. *et al.* ULK1.ATG13.FIP200 complex mediates mTOR signaling and is essential for autophagy. *J. Biol. Chem.* **284**, 12297–12305 (2009).
20. Jung, C.H. *et al.* ULK-Atg13–FIP200 complexes mediate mTOR signaling to the autophagy machinery. *Mol. Biol. Cell* **20**, 1992–2003 (2009).
21. Itakura, E. & Mizushima, N. Characterization of autophagosome formation site by a hierarchical analysis of mammalian Atg proteins. *Autophagy* **6**, 764–776 (2010).
22. Hara, T. *et al.* FIP200, a ULK-interacting protein, is required for autophagosome formation in mammalian cells. *J. Cell Biol.* **181**, 497–510 (2008).
23. Mizushima, N. *et al.* Mouse Apg16L, a novel WD-repeat protein, targets to the autophagic isolation membrane with the Apg12-Apg5 conjugate. *J. Cell Sci.* **116**, 1679–1688 (2003).
24. Fujioka, Y., Noda, N.N., Nakatogawa, H., Ohsumi, Y. & Inagaki, F. Dimeric coiled-coil structure of *Saccharomyces cerevisiae* Atg16 and its functional significance in autophagy. *J. Biol. Chem.* **285**, 1508–1515 (2010).
25. Matsushita, M. *et al.* Structure of Atg5Atg16, a complex essential for autophagy. *J. Biol. Chem.* **282**, 6763–6772 (2007).
26. Ishibashi, K. *et al.* Atg16L2, a novel isoform of mammalian Atg16L that is not essential for canonical autophagy despite forming an Atg12–5-16L2 complex. *Autophagy* **7**, 1500–1513 (2011).
27. Cheong, H., Lindsten, T., Wu, J., Lu, C. & Thompson, C.B. Ammonia-induced autophagy is independent of ULK1/ULK2 kinases. *Proc. Natl. Acad. Sci. USA* **108**, 11121–11126 (2011).
28. Eng, C.H., Yu, K., Lucas, J., White, E. & Abraham, R.T. Ammonia derived from glutaminolysis is a diffusible regulator of autophagy. *Sci. Signal.* **3**, ra31 (2010).
29. Shang, L. *et al.* Nutrient starvation elicits an acute autophagic response mediated by Ulk1 dephosphorylation and its subsequent dissociation from AMPK. *Proc. Natl. Acad. Sci. USA* **108**, 4788–4793 (2011).
30. Alers, S. *et al.* Atg13 and FIP200 act independently of Ulk1 and Ulk2 in autophagy induction. *Autophagy* **7**, 1423–1433 (2011).
31. Kundu, M. *et al.* Ulk1 plays a critical role in the autophagic clearance of mitochondria and ribosomes during reticulocyte maturation. *Blood* **112**, 1493–1502 (2008).
32. Wei, H. *et al.* Suppression of autophagy by FIP200 deletion inhibits mammary tumorigenesis. *Genes Dev.* **25**, 1510–1527 (2011).
33. Fujita, N. *et al.* Differential involvement of Atg16L1 in Crohn disease and canonical autophagy: analysis of the organization of the Atg16L1 complex in fibroblasts. *J. Biol. Chem.* **284**, 32602–32609 (2009).
34. Rioux, J.D. *et al.* Genome-wide association study identifies new susceptibility loci for Crohn disease and implicates autophagy in disease pathogenesis. *Nat. Genet.* **39**, 596–604 (2007).
35. Hampe, J. *et al.* A genome-wide association scan of nonsynonymous SNPs identifies a susceptibility variant for Crohn disease in ATG16L1. *Nat. Genet.* **39**, 207–211 (2007).
36. Hanada, T. *et al.* The Atg12-Atg5 conjugate has a novel E3-like activity for protein lipidation in autophagy. *J. Biol. Chem.* **282**, 37298–37302 (2007).